

Supporting Information

**Bandgap Engineering of Lead-Free Double Perovskites for
Efficient Photocatalysis**

Jinyang Bi¹†, Huijun Lv¹†, Hengguang Wang¹, Liping Du¹, Yan Liu¹, Yueqi Shen¹,
Bo Wu², Yong Wang³, Weihua Ning^{1,4*}

¹*Jiangsu Key Laboratory for Carbon-Based Functional Materials & Devices, Institute of Functional Nano & Soft Materials (FUNSOM), Soochow University, Suzhou, 215123 P. R. China.*

²*Guangdong Provincial Key Laboratory of Optical Information Materials and Technology and Institute of Electronic Paper Displays, South China Academy of Advanced Optoelectronics, South China Normal University, Guangzhou 510006, P. R. China.*

³*State Key Laboratory of Silicon and Advanced Semiconductor Materials and School of Materials Science and Engineering, Hangzhou Global Scientific and Technological Innovation Center, Zhejiang University, Hangzhou, Zhejiang 310027, P. R. China.*

⁴*Jiangsu Key Laboratory of Advanced Negative Carbon Technologies, Soochow University, Suzhou, 215123, Jiangsu, PR China.*

* Corresponding author. Email: whning@suda.edu.cn

† These authors contributed equally to this work

Methods

Materials

Caesium chloride (CsCl, 99.9%), silver chloride (AgCl, 99.9%), bismuth chloride (BiCl₃, 99.9%), antimony pentoxide (Sb₂O₅, 99.5%), antimony chloride (SbCl₃, 99.9%), hydrochloric acid (HCl, 37 wt.% in water), hypophosphorous acid (H₃PO₂, 50 wt.% solution in water) and isopropyl alcohol were purchased from Aladdin. All the aforementioned chemical reagents were utilized directly without undergoing any purification process.

Sample characterizations

UV-Vis absorption spectra were measured in solid integrating sphere mode with a UV-Vis-IR spectrophotometer (UV 3600). The PXRD measurement method involved grinding the SCs into powders in a mortar, XRD patterns of the products were recorded with an X-ray diffractometer (Empyrean) using Cu K α radiation, operating at 40 KV and 40 mA. The PL spectrum was measured using a Fluoromax-4 fluorescence spectrophotometer excited by 300 nm output of a continuous xenon lamp (Xe 900). The excitation slit width was set at 5 nm, the detection slit width was set at 1.75 nm, and the spectra were recorded with 2 nm steps. The time-resolved photoluminescence (TRPL) measurement was performed using a fluorescence spectrometer (PL-TCSPEC). The XPS was carried out on the AXIS Supra+ spectrometer. ICP-MS measurements were performed on a NexION 350X spectrometer. All chemical analyses performed by ICP-MS were subject to a systematic error of \approx 5%. SEM and EDX mapping were carried out on a scanning electron microscope (ZEISS G500).

Synthesis of Double Perovskite Single Crystals (SCs)

CsCl (168.300 mg, 1 mmol), AgCl (71.660 mg, 0.5 mmol) and BiCl₃ (122.635 mg, 0.5 mmol) were dissolved in 6 ml of hydrochloric acid with 10 ml of Teflon lined. The container was then transferred into a X mL Teflon-lined stainless steel

autoclave and kept in an oven at 180 °C for 12 hours. Next, the solution was slowly cooled to room temperature at a rate of 3 °C h⁻¹. The obtained SCs were filtered out and washed with isopropanol. Finally, then dried in an oven 60 °C for 3 h. Sb-doped SCs were prepared by the same protocol but with the addition of Sb₂O₅ and SbCl₃ (x mmol, x = 0.1, 0.2 and 0.3). The synthetic scheme for the introduction of the reducing agent was the same but 10 µl of H₃PO₂ was added before transferring the container to the Teflon-lined stainless steel autoclave.

Photocatalytic H₂ Production Measurements

The photocatalytic H₂ evolution in an aqueous HCl/H₃PO₂ (HCl : H₃PO₂ = 5:1 in volume ratio) solution was carried out in a quartz vessel connected to a closed gas circulation irradiated with 300 W Xe lamp (CEL-HXF300-T3) with UVCUT-420, UVCUT-500 and UVCUT-700 filters. The light intensity is about 100 mW cm⁻² measured using a thermopile sensor (Newport, Model 818P-001-12) and light irradiation area was controlled by masking the surface of the reactor. In a typical photocatalytic experiment, 10 mg of as-synthesized photocatalyst was added into 15 mL HCl/H₃PO₂ saturated solution and stirred for 30 min in the photocatalytic reactor to evenly disperse the catalyst while vacuuming for driving off the air inside. The temperature of the reactor was maintained at 25 °C by a cooling water system. The generated H₂ was quantified using online gas chromatograph (Shimadzu GC 2014, TCD, Ar carrier). The amount of evolved H₂ was detected every half hour in a 4 h test.

Photoelectrochemical Measurements

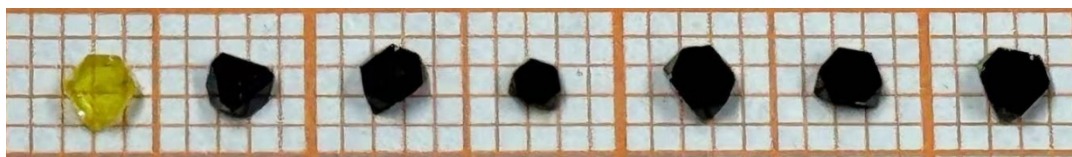
All the photoelectrochemical characterizations were carried out on a CHI660C electrochemical analyzer with a conventional three-electrode system: a gauze platinum as the counter electrode, an Ag/AgCl electrode (3 M KCl) as the reference electrode. The dichloromethane with 0.1 M tetrabutylammonium hexafluorophosphate (TBAPF₆) was filled in the cell as an electrolyte. The working electrodes were prepared by the spin-coating method. The precursor solution was

obtained by adding an excess amount of powder samples into a mixture of anhydrous ethanol and Nafion to make them supersaturated. Specifically, 50 mg sample was dispersed in a mixture of 40 μ l Nafion and 960 μ l anhydrous ethanol with the assistance of ultrasonication. The obtained paste was spin-coated on ITO (1*1.2 cm²) with a 1 cm² area and annealed at 100 °C for 1 h to get a homogenous film. EIS signals of as-prepared samples were collected under the open-circuit voltage within the frequency scope of 105-0.1 Hz with a 5mV amplitude sinusoidal perturbation.

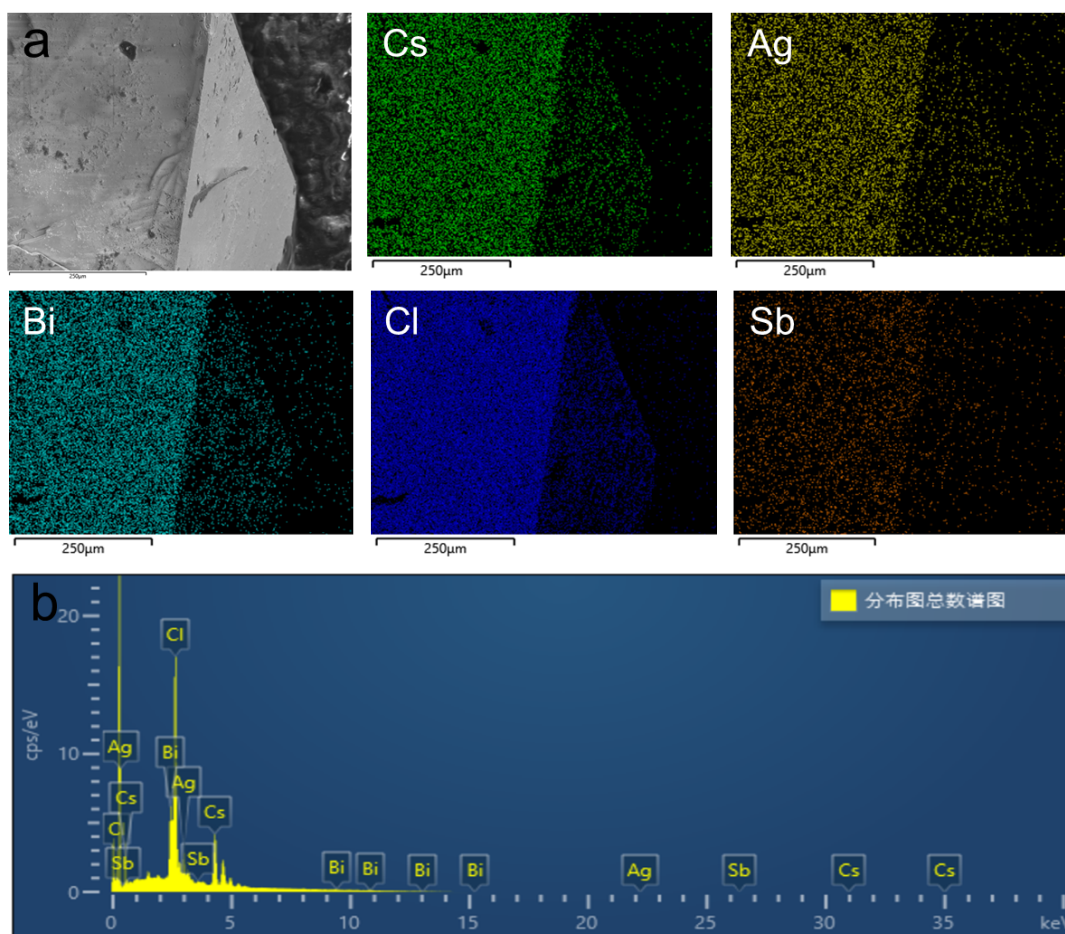
Apparent Quantum Efficiency Measurements

The wavelength-dependent hydrogen evolution efficiency of Cs₂AgBiBr₆:0.63% Sb⁵⁺ has been tested following a similar procedure of photocatalytic H₂ evolution, except that the band-pass filter was equipped to obtain monochromatic incident light (λ =420, 450, 475, 500, 550, 600, 650 and 700 nm). The apparent quantum efficiency (AQE) was calculated from equation:

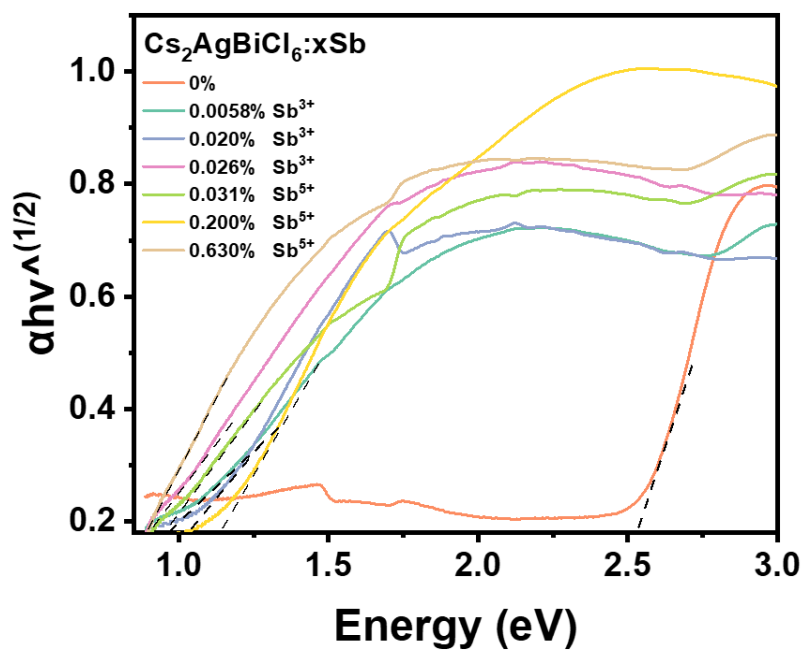
$$AQE = \frac{2 \times \text{number of evolved H}_2 \text{ molecules}}{\text{the number of incident photon}} \times 100\%$$



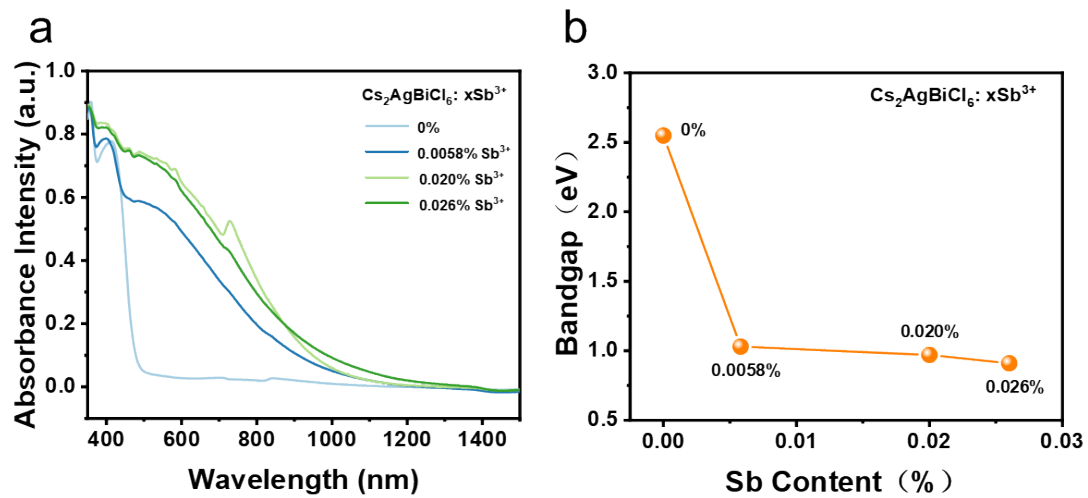
Supplementary Fig. 1 Optical images of $\text{Cs}_2\text{AgBiCl}_6: x\text{Sb}$ ($x= 0.0058\% \text{Sb}^{3+}$,
 $0.020\% \text{Sb}^{3+}$, $0.026\% \text{Sb}^{3+}$, $0.031\% \text{Sb}^{5+}$, $0.200\% \text{Sb}^{5+}$, $0.630\% \text{Sb}^{5+}$)



Supplementary Fig. 2 (a) SEM image and SEM-EDX mapping of Cs, Ag, Bi, Cl, and Sb elements in $\text{Cs}_2\text{AgBiCl}_6: 0.026\% \text{Sb}^{3+}$ SCs and (b) their spectrogram of the total number of distribution maps.

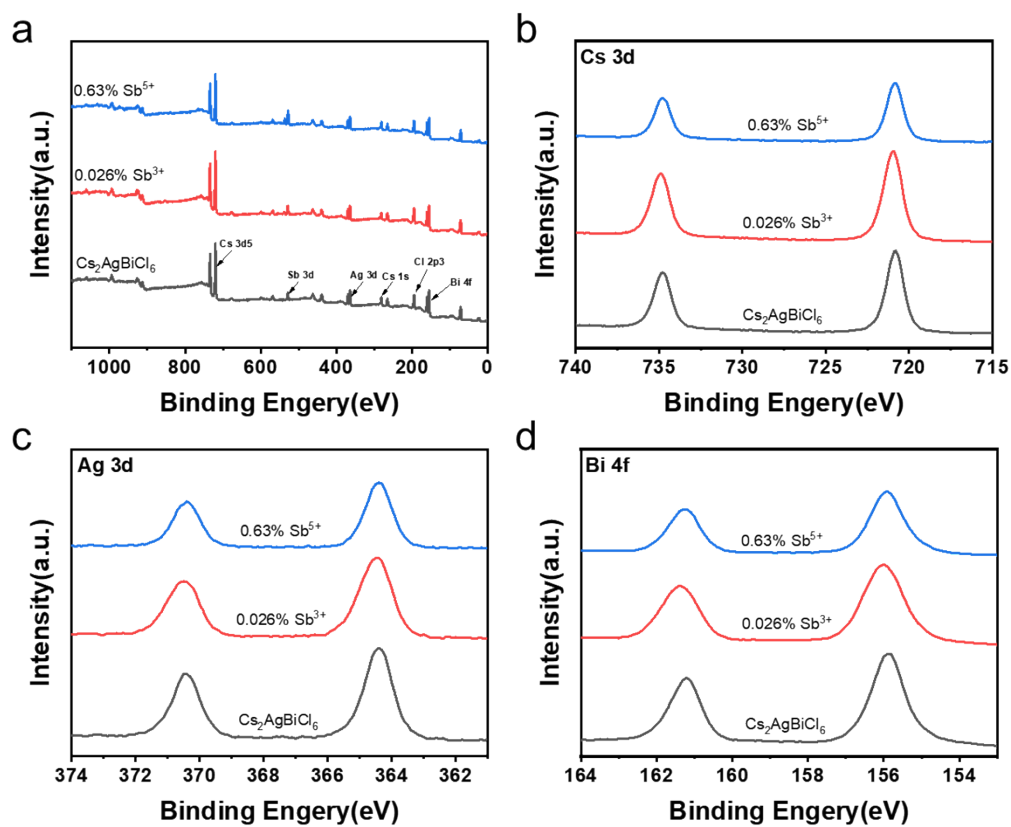


Supplementary Fig. 3 Corresponding indirect Tauc plots of Cs₂AgBiCl₆: xSb.

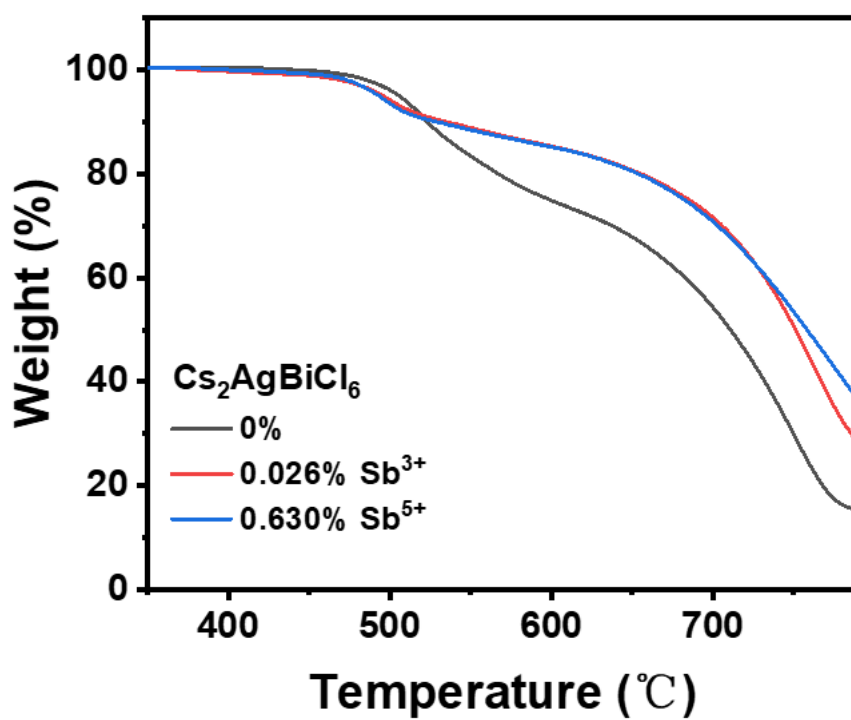


Supplementary Fig. 4 (a) Normalized UV-vis absorption of Cs₂AgBiCl₆: xSb³⁺. **(b)**

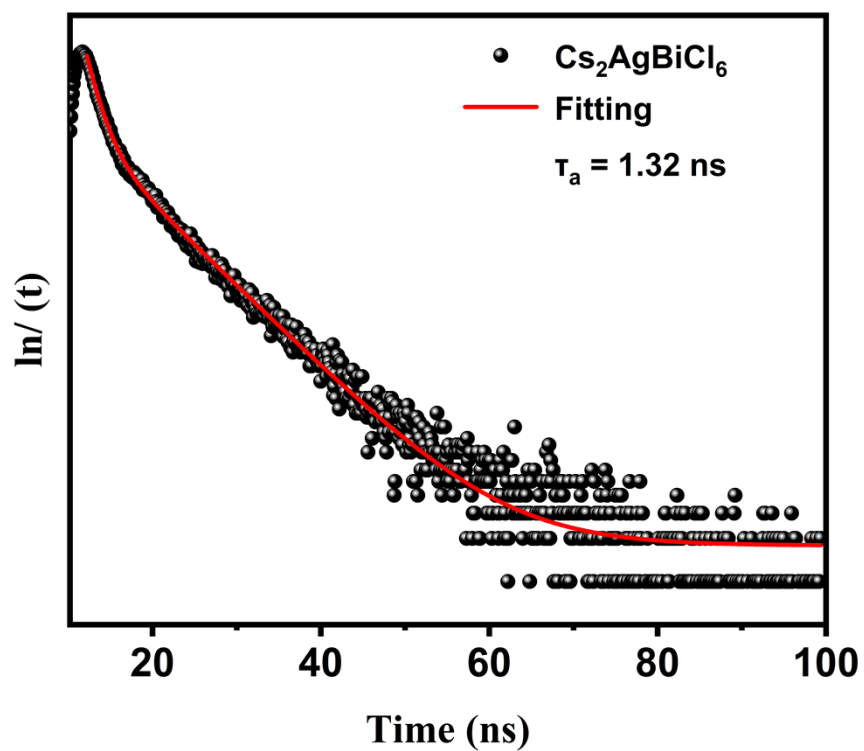
Indirect band gap varies with Sb content.



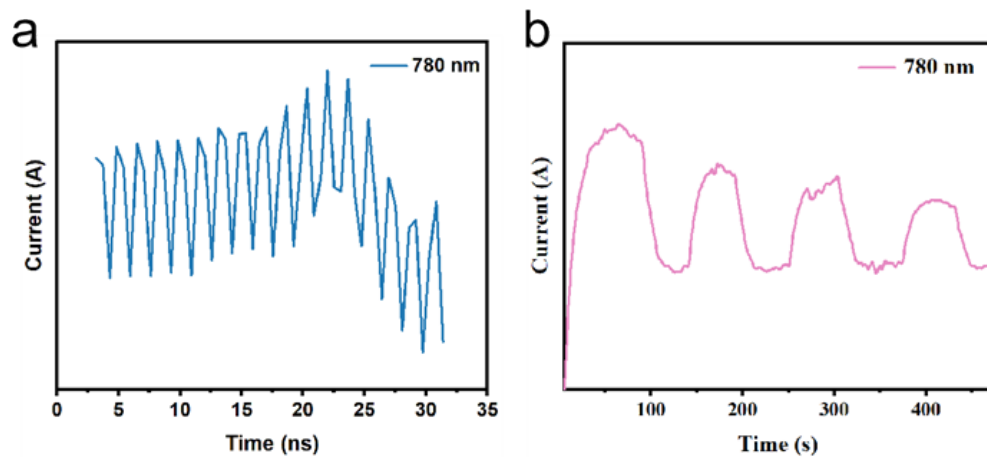
Supplementary Fig. 5 X-ray photoelectron spectroscopy (XPS) spectra of $\text{Cs}_2\text{AgBiCl}_6$, $\text{Cs}_2\text{AgBiCl}_6: 0.026\% \text{Sb}^{3+}$ and $\text{Cs}_2\text{AgBiCl}_6: 0.630\% \text{Sb}^{5+}$.



Supplementary Fig. 6 Thermogravimetric analysis (TGA) spectra of $\text{Cs}_2\text{AgBiCl}_6$,
 $\text{Cs}_2\text{AgBiCl}_6$: 0.026% Sb^{3+} and $\text{Cs}_2\text{AgBiCl}_6$: 0.630% Sb^{5+} .



Supplementary Fig. 7 Time-dependent fluorescence (TRPL) decay curves of $\text{Cs}_2\text{AgBiCl}_6$.



Supplementary Fig. 8 Transient photocurrents at 780 nm of (a) $\text{Cs}_2\text{AgBiCl}_6$ and (b) $\text{Cs}_2\text{AgBiCl}_6: 0.63\% \text{Sb}^{5+}$

Supplementary Table 1. Inductively coupled plasma-Mass Spectrometry (ICP-MS) of Cs₂AgBiCl₆: xSb.

Samples	Sb(ug/L)	W_{Sb}(%)
0.0058% Sb³⁺	7	0.0009
0.0200% Sb³⁺	23	0.0030
0.0260% Sb³⁺	41	0.0032
0.0310% Sb⁵⁺	71	0.0048
0.2000% Sb⁵⁺	427	0.0307
0.6300% Sb⁵⁺	997	0.0968

Supplementary Table 2. The exact location of the XPS peak of the doping samples.

Cs₂AgBiCl₆: 0.026% Sb³⁺ (eV)	Sb⁵⁺	Sb³⁺	O 1s	Sb³⁺	Sb⁵⁺
537.94	536.84	529.24	527.41	528.79	

Cs₂AgBiCl₆: 0.630% Sb⁵⁺ (eV)	Sb⁵⁺	O 1s	Sb⁵⁺
536.93	529	527.78	

Supplementary Table 3. The exact location of the XPS peak of the Sb^{3+} -doped sample with H_3PO_2 .

Sb^{3+}	O 1s	Sb^{3+}
536.87 eV	528.8 eV	527.44 eV

Supplementary Table 4. Fitting Parametric Decay Dynamics to Time-Resolved Concentration Data Using Triple-Exponential Decay Dynamics

	$\tau_1(\text{ns})$	$A_1(\%)$	$\tau_2(\text{ns})$	$A_2(\%)$	$\tau_3(\text{ns})$	$A_3(\%)$	R^2
$\text{Cs}_2\text{AgBiCl}_6$	0.02	7.07	50.20	1.32	49.78	1.32	0.93
$\text{Cs}_2\text{AgBiCl}_6: 0.026\% \text{Sb}^{3+}$	0.058	11.19	50.76	1.25	49.19	1.40	0.97
$\text{Cs}_2\text{AgBiCl}_6: 0.630\% \text{Sb}^{5+}$	0.26	7.01	50.66	1.48	49.07	1.48	0.98

Calculation method for average PL lifetime

The average PL lifetime can be determined by the following equation :

$$x = \frac{A_1 * \tau_1 * \tau_1 + A_2 * \tau_2 * \tau_2 + A_3 * \tau_3 * \tau_3}{\tau_1 * A_1 + \tau_2 * A_2 + \tau_3 * A_3}$$

References

1. H. Yin, J. Chen, P. Guan, D. Zheng, Q. Kong, S. Yang, P. Zhou, B. Yang, T. Pullerits and K. Han, *Angew Chem Int Ed*, 2021, **60**, 22693–22699.
2. C. Yuan, H. Yin, H. Lv, Y. Zhang, J. Li, D. Xiao, X. Yang, Y. Zhang and P. Zhang, *JACS Au*, 2023, **3**, 3127–3140.
3. H. Lv, H. Yin, N. Jiao, C. Yuan, S. Weng, K. Zhou, Y. Dang, X. Wang, Z. Lu and Y. Zhang, *Small Methods*, 2023, **7**, 2201365.
4. Y. Liu, X. Dai, X. Zeng, X. Yuan, Y. Wang, Y. Song, H. Chen, C. Zhang, Y. Wang, L. Wan, Y. Zou, W. Ning and B. Sun, *Adv. Opt. Mater.*, 2024, **12**, 2301576.
5. Z. Cui, Y. Wu, S. Zhang, H. Fu, G. Chen, Z. Lou, X. Liu, Q. Zhang, Z. Wang, Z. Zheng, H. Cheng, Y. Liu, Y. Dai, B. Huang and P. Wang, *Chemical Engineering Journal*, 2023, **451**, 138927.
6. G. Chen, P. Wang, Y. Wu, Q. Zhang, Q. Wu, Z. Wang, Z. Zheng, Y. Liu, Y. Dai and B. Huang, *Adv. Mater.*, 2020, **32**, 2001344.
7. J. Lee, W. Chong, S. H. W. Kok, B. Ng, X. Y. Kong, S. Chai and L. Tan, *Adv. Funct. Mater.*, 2023, **33**, 2303430.
8. M. Shi, P. Fu, W. Tian, H. Chi, C. Li and R. Li, *Small Methods*, 2024, **8**, 2300405.